Solvent Extraction Research and Development, Japan, **Vol. 14, 133 - 144 (2007)**

Role of Zn(II) and Pyridyl Groups in the Adsorption and Self-Aggregation of Zinc Tetrapyridylporphine at the Liquid-Liquid Interface

Hideaki TAKECHI and Hitoshi WATARAI*
Department of Chemistry, Graduate School of Science,
Osaka University, Toyonaka, Osaka 560-0043, Japan

Role of Zn(II) and pyridyl groups in the interfacial adsorption and self-aggregation of zinc 5,10,15,20-tetra(4-pyridyl)-21*H*,23*H*-porphine (ZnTPyP) at the toluene/water system including 5% chloroform finally was investigated by high-speed stirring (HSS) and centrifugal liquid membrane (CLM) methods. At first, the interfacial adsorptivity of ZnTPyP was examined in the absence and presence of pyridine. From experimental results, it was found that the interfacial adsorption and the aggregation of ZnTPyP was remarkably prevented by the adduct formation of ZnTPyP-pyridine complex in the toluene phase, and the adduct formation constants in toluene were determined. Secondly, it was observed that the interfacial adsorptivity and aggregate formation of the ZnTPyP analogues, 5,10,15,20-tetra(4-pyridyl)-21*H*,23*H*-porphine (TPyP) and 5,10,15,20-tetraphenyl-21*H*,23*H*-porphine zinc (ZnTPP), were all less than those for ZnTPyP. Then, it was confirmed that the interfacial self-aggregate of ZnTPyP was formed by the bonding of central zinc atom of ZnTPyP with pyridyl groups of adjacent ZnTPyP molecules.

1. Introduction

Interfacial nanochemistry is growing as a new field in relation to analytical, separation, synthetic and molecular simulation sciences [1]. Determination of the structure of adsorbed species at the liquid-liquid interface is highly important in the study of kinetic mechanisms of solvent extraction and enzymatic reaction mechanisms at bio-membranes [2]. At the liquid-liquid interface, it is expected that a molecular aggregate, which is not formed in bulk phase, can be formed easily, because the interfacial concentration of a surface active monomer becomes much higher than that in a bulk phase. Recently, the aggregation behavior of some phthalocyanine and porphyrin molecules has been studied at the liquid-liquid interface

using various techniques including a high-speed stirring (HSS) method [3], a centrifugal liquid membrane (CLM) method [3-5], a quasi-elastic laser scattering [6], a reflection spectroscopy [7,8] and a second-harmonic generation spectrometry [5,6,9]. The interfacial aggregation of zinc 5,10,15,20-tetra(4-pyridyl)-21*H*,23*H*-porphine (ZnTPyP) has been suggested by the CLM measurement [10]. However, further experimental evidences were required to clarify the structure and the bonding interaction in the self-aggregate of ZnTPyP formed at the liquid-liquid interface. In the present study, the interfacial adsorptivity and the aggregation of ZnTPyP at the liquid-liquid interface were investigated by using HSS and CLM methods in the absence and presence of pyridine. Furthermore, the interfacial behavior of the ZnTPyP analogues, 5,10,15,20-tetra(4-pyridyl)-21*H*,23*H*-porphine (TPyP) and 5,10,15,20-tetraphenyl-21*H*,23*H*-porphine zinc (ZnTPP), were examined to clarify the role of the central zinc atom and the pyridyl group in the interfacial adsorption and the interfacial aggregation of ZnTPyP.

2. Experimental

2.1 Reagents.

Zinc 5,10,15,20-tetra(4-pyridyl)-21*H*,23*H*-porphine (ZnTPyP, Figure 1), 5,10,15,20-tetra(4-pyridyl)-21*H*,23*H*-porphine (TPyP) and sodium perchlorate (GR grade) were purchased from Aldrich (USA). 5,10,15,20-Tetraphenyl-21*H*,23*H*-porphine zinc (ZnTPP) was purchased from SIGMA-ALDRICH (USA). Toluene, chloroform and pyridine were purchased from Nacalai Tesque Inc. (Kyoto, Japan) and used as received. Toluene was a poor solvent for ZnTPyP. Therefore, in the HSS and CLM experiments, toluene including 5% chloroform was used as an organic phase solvent. Chloroform was used to prepare the stock solution of porphyrins. Water was distilled and deionized by a Milli-Q system (Millipore, USA).

2.2 High-Speed Stirring Measurement.

The interfacial adsorption of the porphyrins in the liquid-liquid interface was measured by using a high-speed stirring (HSS) method. The principle of HSS method was described elsewhere [11], and an

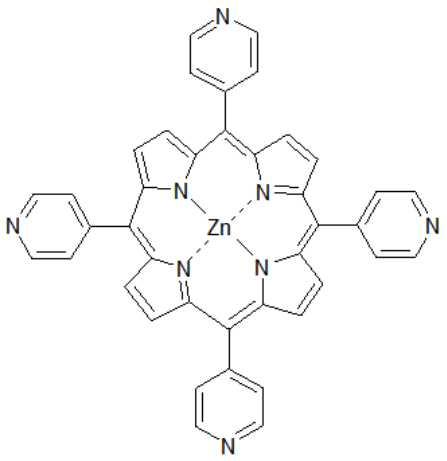

Figure 1. Molecular structure of ZnTPyP

analogous procedure was employed in the present study [12-14]. Briefly, 50 mL toluene including 2.5 mL chloroform and the aqueous phase adjusted 0.1 M ionic strength by $NaClO_4$ (50 mL) were agitated at a stirring rate of 5000 and 200 rpm in the glass stir cell, and a stock solution of a porphyrin in chloroform less than 300 μL was added before measurement. The organic phase was continuously separated from the agitated mixture by means of a PTFE phase separator, and circulated through a flow cell at a flow rate of ca. 20 mL min^{-1} by an electric pump (Flumax Junior, Fluid Metering Inc., Japan). Absorption spectra of the separated organic phase were measured in the range of 300-800 nm using a photodiode-array UV-vis detector (SPD-M 6A, Shimadzu, Japan). The interfacial concentration of porphyrins could be determined from the difference between the absorbances of the organic phase under a high-speed stirring (5000 rpm) and a low-speed stirring (200 rpm) conditions at the absorption maximum wavelength.

The adsorption isotherm of porphyrin was measured by the HSS method using various concentrations of porphyrins. For the analysis of the observed isotherm, the Langmuir isotherm was applied [15],

$$[\mathrm{Pr}]_i = \frac{aK'[\mathrm{Pr}]_o}{a + K'[\mathrm{Pr}]_o} \quad (1)$$

where $[Pr]_i$ and $[Pr]_o$ denote the concentrations of a porphyrin adsorbed at the liquid-liquid interface (mol/dm^2) and in the bulk toluene phase (mol/dm^3), respectively. a is the saturated interfacial concentration (mol/dm^2) and K' is the interfacial adsorption constant (dm) defined at an infinitely diluted concentration of porphyrin,

$$K' = \frac{[\mathrm{Pr}]_i}{[\mathrm{Pr}]_o} \quad (2)$$

The difference between the absorbances of bulk organic phase under high-speed stirring and low-speed stirring conditions, ΔA, and the absorbance of the bulk organic phase under the high-speed stirring, A_o, can be described as follows,

$$\Delta A = \varepsilon l [\mathrm{Pr}]_i \frac{S_i}{V_o} \quad (3)$$

$$A_o = \varepsilon l [\mathrm{Pr}]_o \quad (4)$$

where ε, l, S_i and V_o are the molar absorptivity in the organic phase (toluene/chloroform = 95/5, v/v), the optical path length, the total interfacial area, and the organic phase volume, respectively. Total interfacial area was reported to be 2.0×10^2 dm^2 [16].

2.3 UV-Vis Absorption Spectra of the Liquid Membrane System.

The interfacial formation of ZnTPyP self-aggregate was directly measured spectrophotometrically by the centrifugal liquid membrane (CLM) method. The principle of CLM method was described elsewhere [17]. The apparatus for CLM method was essentially the same with that reported previously [18,19]. Briefly, a cylindrical cell, whose height and outer diameter were 3.4 and 1.9 cm, respectively, was placed horizontally in a sample chamber of a diode array UV-vis spectrophotometer (8543, Agilent, USA) and rotated at 10,000 rpm by a speed-controlled motor (NE-22E, Nakanishi Inc., Japan). At first, a blank

spectrum was measured by introducing 0.500 mL aqueous solution of 0.1M $NaClO_4$ (pH5.5) and 0.380 mL toluene by a microsyringe into the cylindrical cell. Then, 0.020 mL chloroform solution of 1.5×10^{-4} M ZnTPyP was added and the self-aggregate formation was initiated. The sum of absorption spectra of bulk phase and the interface was measured. The calculated values of thickness of the organic and aqueous phase were 0.20 and 0.25 mm, respectively. The interfacial area, S_i, between two phases was 20 cm^2.

UV-visible spectra in organic solution were obtained on a V-570 spectrometer (JASCO, Japan). Values of pH of aqueous phases were measured by a F-14 pH meter (HORIBA, Japan) equipped with a 6366-10D glass electrode.

3. Results and Discussion

3.1 Interfacial Adsorption of ZnTPyP at the Liquid-Liquid Interface.

In the high-speed stirring (HSS) experiments with lower concentrations of ZnTPyP than 8.0×10^{-8} mol dm^{-3} in the liquid-liquid system, ZnTPyP showed appreciable adsorption to the interface. The adsorption isotherm was obtained as shown in Figure 2 and was analyzed by eq. (1). From the analysis with Langmuir isotherm, the interfacial constant, *K'*, and the saturated interfacial concentration, *a*, of ZnTPyP were determined as 6.9×10^{-3} dm and 5.6×10^{-10} mol dm^{-2}, respectively.

3.2 Interfacial Self-Aggregation of ZnTPyP at the Liquid-Liquid Interface.

The formation of the self-aggregate of ZnTPyP at the interface was directly measured by the CLM technique. Figure 3 shows the spectral change due to the interfacial self-aggregation of ZnTPyP. It can be seen that low-energy Soret band at 454nm, probably associated with J-type aggregate [20,21], increases gradually, while the high-energy Soret band at 423nm, referred to the monomer, decreases gradually. After about 8 min, the self-aggregation process reached an equilibrium state in the present conditions.

After the measurement, the interfacial self-aggregates of ZnTPyP formed in the CLM cell were transferred on a cover glass. They were observed by an optical microscope, and the image is shown in

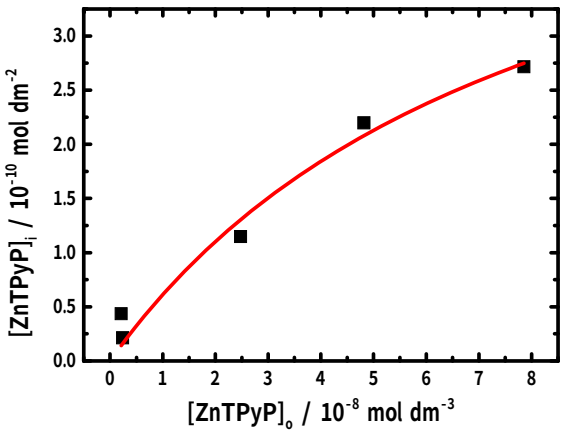

Figure 2. Adsorption isotherm of ZnTPyP measured by the HSS method at the liquid-liquid interface at 25°C. The line is the best fit of the data to eq. (1).

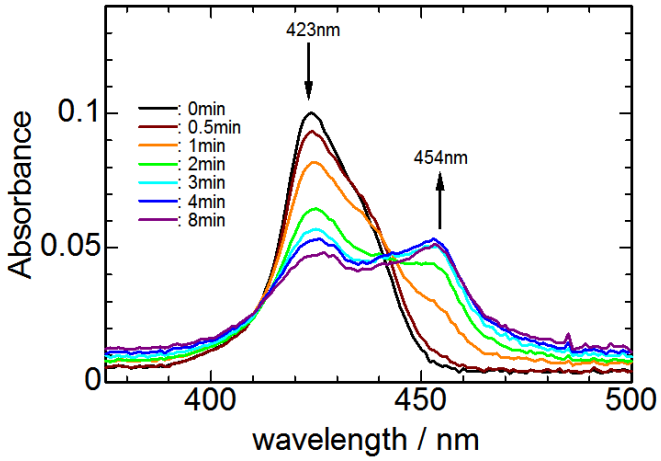

Figure 3. UV-Visible absorption spectral changes due to the interfacial self-aggregation of ZnTPyP at the toluene/water system measured by the CLM technique. Arrows indicate the direction of the absorbance changes with the time course. The initial concentration of ZnTPyP in the organic phase (toluene/chloroform = 95/5, v/v) was 7.5×10^{-6} M, and the concentration of $NaClO_4$ in the aqueous phase was 0.1 M (pH = 5.5).

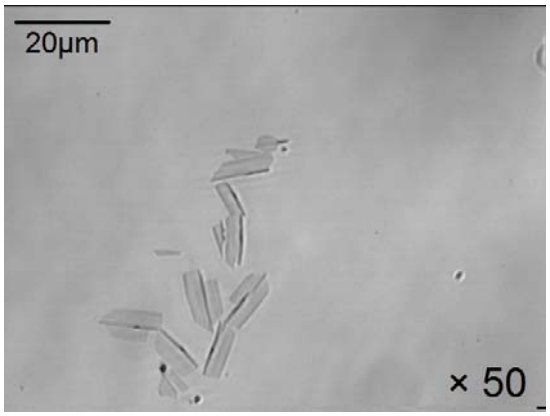

Figure 4. Microscopic image of the interfacial self-aggregates of ZnTPyP transferred on a cover glass after a CLM measurement ($[ZnTPyP]_o = 2.5 \times 10^{-6}$ M).

Figure 4, where the length of the rectangular self-aggregate is ca. 10 μm. The thickness was estimated as ca. 4 nm from the absorbance of the aggregate. When the two phases were transferred in a watch glass after a CLM measurement, the liquid-liquid interface image observed by optical microscope was similar to the above image. But, it was difficult to observe continuously the liquid-liquid interface because of the evaporation of the organic phase.

3.3 Effect of Pyridine on the Interfacial Adsorption of ZnTPyP.

We thought that the interfacial self-aggregate might be formed by the coordination of pyridyl group of one ZnTPyP to the central zinc atom of another ZnTPyP molecule. So, we investigated the effect of

pyridine on the interfacial adsorption of ZnTPyP. When pyridine was added into the organic phase in the HSS and CLM measurements, the interfacial adsorption and the interfacial aggregation of ZnTPyP were remarkably depressed.

To clarify the effect of pyridine on the interfacial adsorption, we examined the reactivity between ZnTPyP and pyridine in the organic phase. We could observe the absorbance increases with the shift of the maximum wavelength from 423 nm to 428 nm, when the pyridine concentration was changed at the fixed initial ZnTPyP concentration ($[ZnTPyP]_o = 2.5 \times 10^{-6}$ M) (Figure 5 (a)). Furthermore, when the concentration of pyridine was changed in the wide range of 5.0×10^{-7} M - 8.0×10^{-3} M, we observed

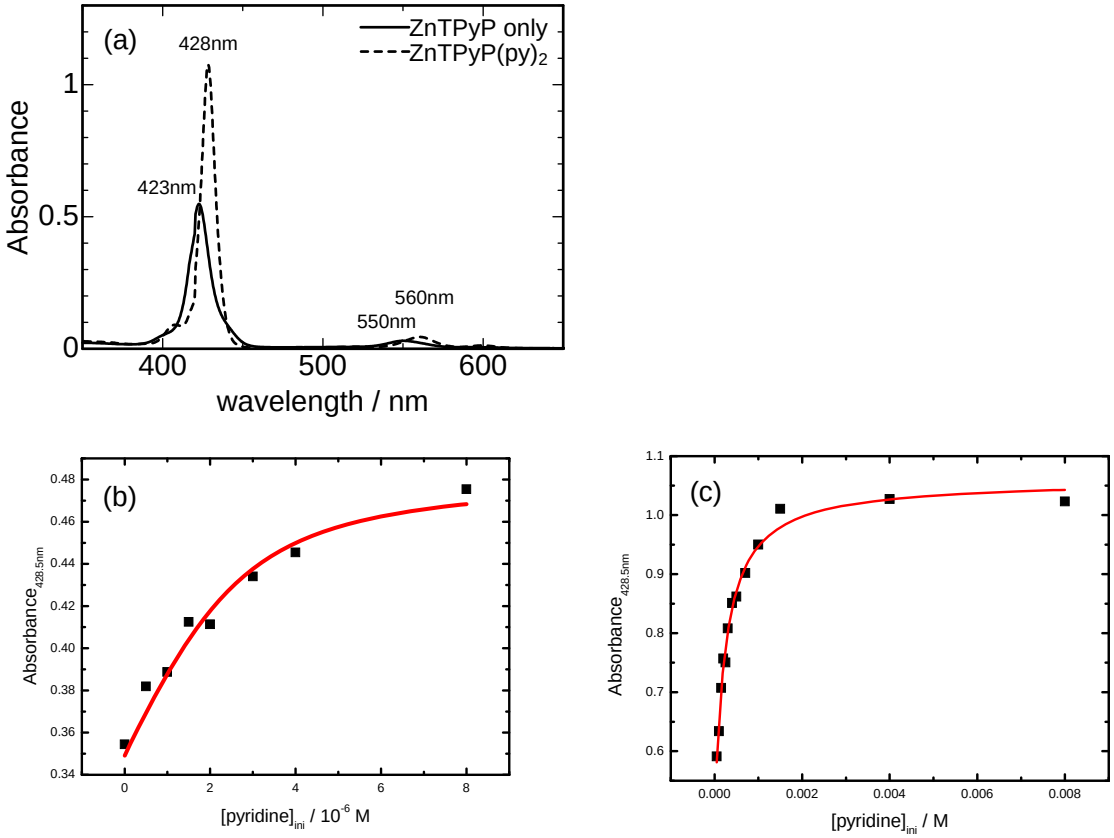

Figure 5. (a) UV-Visible absorption spectra of ZnTPyP (solid line) and $ZnTPyP(py)_2$ complex (dotted line) in the organic solution (toluene/chloroform = 95/5, v/v). Initial concentrations: (solid line) $[ZnTPyP]_o = 2.5 \times 10^{-6}$ M; (dotted line) $[ZnTPyP]_o = 2.5 \times 10^{-6}$ M, $[pyridine]_o = 4.1 \times 10^{-2}$ M. (b) Absorbance changes at 428.5 nm in lower pyridine concentrations. The line is the best fit of the data to the eq. (13). Initial concentrations: $[ZnTPyP]_o = 2.5 \times 10^{-6}$ M, $[pyridine]_o = 0$ - 8.0×10^{-6} M. (c) Absorbance changes at 428.5 nm in higher pyridine concentrations. The line is the best fit of the data to the eq. (17). Initial concentrations: $[ZnTPyP]_o = 2.5 \times 10^{-6}$ M, $[pyridine]_o = 5.0 \times 10^{-5}$ - 8.0×10^{-3} M.

two-step reactions according to the concentration of pyridine. As shown in Figure 5 (b) and 5 (c), we could measure the individual saturation curves in the lower and higher concentration regions of pyridine. The absorbance changes at 428.5nm, the maximum wavelength of ZnTPyP in the highest pyridine concentration, shown in Figure 5 (b) and 5 (c) were analyzed by the next adduct formation reactions between ZnTPyP and pyridine, respectively,

$$\mathrm{ZnTPyP} + \mathrm{pyridine} \overset{K_1}{\rightleftharpoons} \mathrm{ZnTPyPpy} \tag{5}$$

$$\mathrm{ZnTPyPpy} + \mathrm{pyridine} \overset{K_2}{\rightleftharpoons} \mathrm{ZnTPyP(py)_2} \tag{6}$$

where ZnTPyPpy and ZnTPyP(py)$_2$ are one and two pyridine coordinated complexes, respectively. K_1 and K_2 are equilibrium constants for the reactions of (5) and (6), respectively. K_1 and K_2 are defined as follows,

$$K_1 = \frac{[\mathrm{ZnTPyPpy}]}{[\mathrm{ZnTPyP}][\mathrm{pyridine}]} \tag{7}$$

$$K_2 = \frac{[\mathrm{ZnTPyP(py)_2}]}{[\mathrm{ZnTPyPpy}][\mathrm{pyridine}]} \tag{8}$$

where [ZnTPyP], [pyridine], [ZnTPyPpy] and [ZnTPyP(py)$_2$] denote the concentrations (mol dm^{-3}) of ZnTPyP, pyridine, ZnTPyPpy and ZnTPyP(py)$_2$, respectively. The absorbance at 428.5 nm was described as follows,

$$Abs_{428.5} = \varepsilon_{ZnTPyP}[\mathrm{ZnTPyP}] + \varepsilon_{ZnTPyPpy}[\mathrm{ZnTPyPpy}] + \varepsilon_{ZnTPyP(py)2}[\mathrm{ZnTPyP(py)_2}] \tag{9}$$

where ε_{ZnTPyP}, $\varepsilon_{ZnTPyPpy}$ and $\varepsilon_{ZnTPyP(py)2}$ are molar absorptivities (mol^{-1} dm^3 cm^{-1}) at 428.5nm in the organic phase (toluene/chloroform = 95/5, v/v) of ZnTPyP, ZnTPyPpy and ZnTPyP(py)$_2$, respectively.

When pyridine concentration is low, the concentration of ZnTPyP(py)$_2$ is negligibly small. So, concentrations can be approximated as follows,

$$[\mathrm{ZnTPyP(py)_2}] = 0 \tag{10}$$

$$[\mathrm{ZnTPyP}]_{\mathrm{ini}} = [\mathrm{ZnTPyP}] + [\mathrm{ZnTPyPpy}] \tag{11}$$

$$[\mathrm{pyridine}] = [\mathrm{pyridine}]_{\mathrm{ini}} - [\mathrm{ZnTPyPpy}] \tag{12}$$

where [ZnTPyP]$_{\mathrm{ini}}$ and [pyridine]$_{\mathrm{ini}}$ are initial concentrations of ZnTPyP and pyridine, respectively.

From eqs. (9) - (12), eq. (13) is obtained.

$$Abs_{428.5} = \varepsilon_{ZnTPyP}[\mathrm{ZnTPyP}]_{\mathrm{ini}} + (\varepsilon_{ZnTPyPpy} - \varepsilon_{ZnTPyP})[\mathrm{pyridine}]_{\mathrm{ini}} - (\varepsilon_{ZnTPyPpy} - \varepsilon_{ZnTPyP})\frac{-K_1[\mathrm{ZnTPyP}]_{\mathrm{ini}} + K_1[\mathrm{pyridine}]_{\mathrm{ini}} - 1}{2K_1} - (\varepsilon_{ZnTPyPpy} - \varepsilon_{ZnTPyP})\frac{\sqrt{(K_1[\mathrm{ZnTPyP}]_{\mathrm{ini}} - K_1[\mathrm{pyridine}]_{\mathrm{ini}} + 1)^2 + 4K_1[\mathrm{pyridine}]_{\mathrm{ini}}}}{2K_1} \tag{13}$$

The values of ε_{ZnTPyP} and $\varepsilon_{ZnTPyPpy}$ were determined experimentally as 1.4×10^5 mol^{-1} dm^3 cm^{-1} and $2.0\times$

10^5 mol^{-1} dm^3 cm^{-1}.

When pyridine concentration is high, the concentration of ZnTPyP is negligibly small and the concentration of pyridine is approximately equal to the initial concentration of pyridine. So, following equations were postulated.

$$[\mathrm{ZnTPyP}] = 0 \tag{14}$$

$$[\mathrm{ZnTPyP}]_{ini} = [\mathrm{ZnTPyPpy}] + [\mathrm{ZnTPyP(py)_2}] \tag{15}$$

$$[\mathrm{pyridine}] = [\mathrm{pyridine}]_{ini} \tag{16}$$

From eq. (9) and eqs. (14) - (16), eq. (17) was obtained.

$$Abs_{428.5} = \varepsilon_{ZnTPyPpy}[\mathrm{ZnTPyP}]_{ini} + (\varepsilon_{ZnTPyP(py)2} - \varepsilon_{ZnTPyPpy})\frac{[\mathrm{ZnTPyP}]_{ini} K_2 [\mathrm{pyridine}]_{ini}}{1 + K_2[\mathrm{pyridine}]_{ini}} \tag{17}$$

where $\varepsilon_{ZnTPyP(py)2}$ was determined as 4.3×10^5 mol^{-1} dm^3 cm^{-1}.

From eqs. (13) and (17), the equilibrium constants, K_1 and K_2, were calculated to be 1.4×10^6 mol^{-1} dm^3 and 4.1×10^3 mol^{-1} dm^3, respectively.

The spectral changes observed for ZnTPyP was also observed in ZnTPP, but it was not observed in TPyP. Therefore, the coordination of two pyridine molecules to the central zinc atom of ZnTPyP was expected in the 1:2 complex as shown in Figure 6.

Figure 7 (a) shows the Langmuir isotherm for the adsorption of $ZnTPyP(py)_2$ conducted under the excess concentration of pyridine, which gave the interfacial constant, *K'*, and the saturated interfacial concentration, *a*, of $ZnTPyP(py)_2$ as 2.2×10^{-4} dm and 7.6×10^{-11} mol dm^{-2}, respectively. These values are significantly smaller than those of ZnTPyP. This means that the interfacial adsorptivity of ZnTPyP is depressed by the formation of $ZnTPyP(py)_2$ in the organic phase. This is due to the block effect of the central zinc atom by the coordination of pyridine molecules from the hydration of the central zinc atom at the interface. In addition, an increase of hydrophobicity due to the two pyridine molecules will increase its solubility in organic phase. Low-energy Soret band at 454nm observed in J-type ZnTPyP aggregate was not observed in $ZnTPyP(py)_2$ (Figure 7 (b)). It was concluded that the interfacial aggregation of ZnTPyP was depressed by the formation of $ZnTPyP(py)_2$ in the organic phase including pyridine.

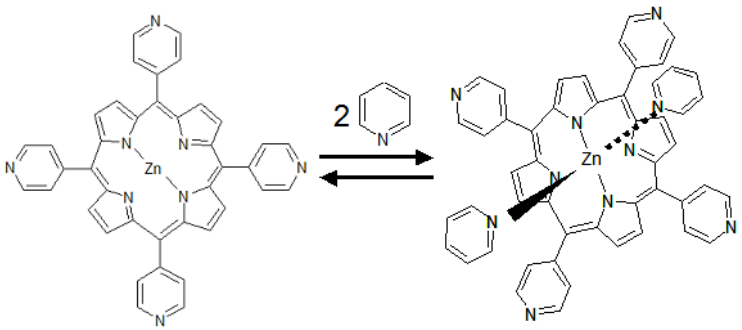

Figure 6. Structure of the adduct of $ZnTPyP(py)_2$ formed in the organic phase.

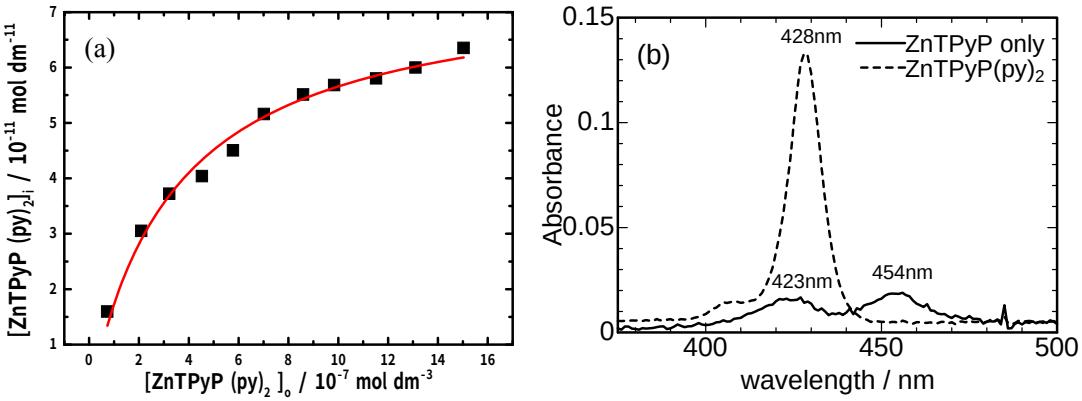

Figure 7. (a) Adsorption isotherm of $ZnTPyP(py)_2$ measured by the HSS method at the liquid-liquid interface at 25°C. The line is the best fit of the data to eq (1). Initial concentrations: $[ZnTPyP]_o = 2.5 \times 10^{-7}$ - 3.0×10^{-6} M, $[pyridine]_o = 6.3 \times 10^{-3}$ - 7.5×10^{-2} M, $[ZnTPyP]_o/[pyridine]_o = 1/25000$. (b) UV-Visible absorption spectra of ZnTPyP (solid line) and $ZnTPyP(py)_2$ (dotted line) measured by the CLM method. Concentrations: (solid line) $[ZnTPyP]_o = 5.0 \times 10^{-6}$ M; (dotted line) $[ZnTPyP]_o = 5.0 \times 10^{-6}$ M $[pyridine]_o = 0.30$ M.

3.4 Comparison of Adsorption Behavior of ZnTPyP Analogues at the Liquid-Liquid Interface.

To confirm further the chemical bonding between ZnTPyP molecules in the self-aggregate formed at the liquid-liquid interface, interfacial adsorptivity of ZnTPyP analogue compounds, TPyP and ZnTPP (Figure 8), were evaluated by HSS and CLM methods. The interfacial adsorption constant, *K'*, obtained by HSS measurement and the ability of interfacial self-aggregate evaluated by CLM measurement are summarized in Table 1. It was found that TPyP, that has no central zinc atom, and $ZnTPyP(py)_2$, whose central zinc atom is blocked by pyridine, were less adsorptive to the interface and gave no interfacial self-aggregate. ZnTPP, that has no pyridyl group, also formed no interfacial self-aggregate, though it showed interfacial adsorptibity a little. It was confirmed that central zinc atom and pyridyl group are key of the formation of interfacial self-aggregate of ZnTPyP. It can be concluded that the interfacial self-aggregate of ZnTPyP is formed by the bonding of zinc and pyridyl group as shown in Figure 9, which has been found in the crystal

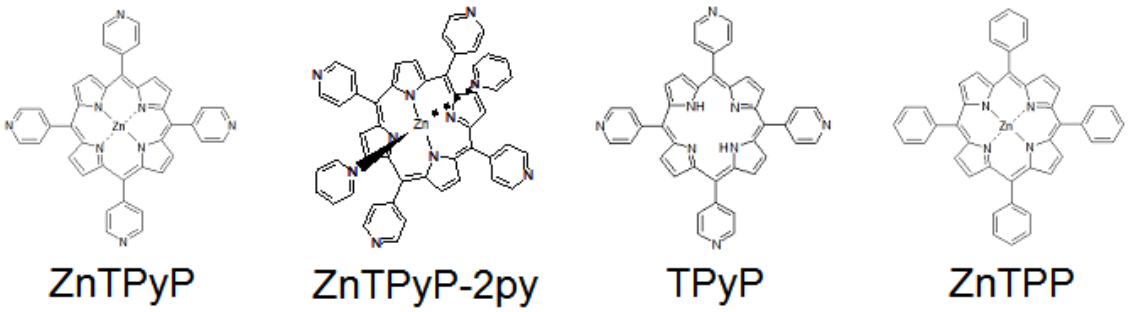

Figure 8. Molecular structures of ZnTPyP, $ZnTPyP(py)_2$, TPyP and ZnTPP

structure of ZnTPyP [22]. Recently, it has been reported that ZnTPyP could form tube-like aggregates in bulk aqueous solution through the bonding of zinc and pyridyl group [23].

Table 1. Interfacial adsorption constant, *K'*, and the ability of the interfacial self-aggregation of ZnTPyP, ZnTPyP(py)$_2$, TPyP and ZnTPP in the liquid-liquid interface measured by the high speed stirring and the centrifugal liquid membrane methods. The organic phase was porphyrin solution (toluene/chloroform = 95/5, v/v) and the aqueous phase was adjusted 0.1 M ionic strength by $NaClO_4$.

	Interfacial Adsorption Constant *K'* / dm	Interfacial Self-Aggregates
ZnTPyP	6.9×10^{-3}	Formed
ZnTPyP(py)$_2$	2.2×10^{-4}	Not Formed
TPyP	5.0×10^{-5}	Not Formed
ZnTPP	$< 10^{-6}$	Not Formed

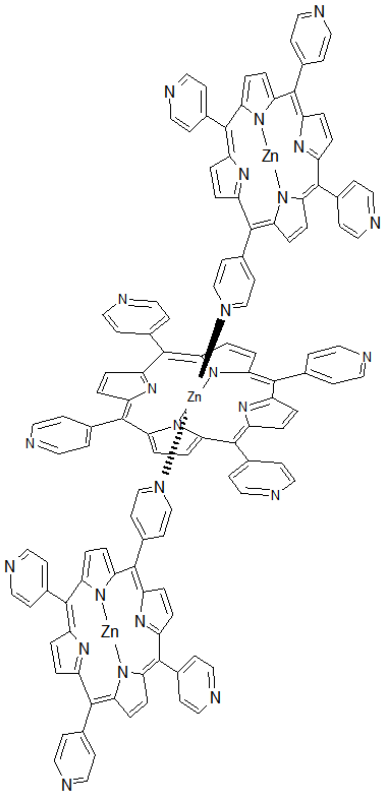

Figure 9. Zn(II)-pyridyl interaction confirmed in the interfacial aggregate of ZnTPyP.

4. Conclusion

The interfacial adsorption and self-aggregation of ZnTPyP at the liquid-liquid interface was investigated by HSS and CLM methods. The role of the central zinc atom and pyridyl groups was clarified in the interfacial adsorption and the interfacial self-aggregation. The interfacial self-aggregate of ZnTPyP formed ca. 10 μm flat structure, whose shape was quadrangle. The study on the fine structure of the interfacial ZnTPyP aggregate is now on going by means of AFM.

Acknowledgment

This study was supported by the Grant-in-Aid for Scientific Research (S) (No. 16105002) and in part by "Special Coordination Funds for Promoting Science and Technology: Yuragi Project" of the Ministry of Education, Culture, Sports, Science and Technology, Japan.

Reference

1) H. Watarai, N. Sawada (eds.), "*Interfacial Nanochemistry*", Kluwer Academic/Plenum Publishers, New York, 2005.

2) A. G. Volkov, D.W. Deamer, D. L. Tanelian, V. S. Markin (eds.), *Liquid interface in Chemistry and Biology*, Wiley, New York, 1998.

3) K. Adachi, K. Chayama, H. Watarai, *Langmuir*, **22**, 1630 (2006).

4) K. Adachi, K. Chayama, H. Watarai, *Chirality*, **18**, 599 (2006).

5) H. Watarai, S. Wada, K. Fujiwara, *Tsinghua Science and Technology*, **11**, 228 (2006).

6) H. Nagatani, Z. Samec, P. F. Brevet, D. J. Fermin, H. H. Girault, *J. Phys. Chem. B*, **107**, 786 (2003)

7) Y. Moriya, T. Hasegawa, K. Hayashi, M. Maruyama, S. Nakata, N. Ogawa, *Anal. Bioanal. Chem.*, **376**, 374 (2003)

8) Y. Moriya, S. Nakata, H. Morimoto, N. Ogawa, *Anal. Sci*., **20**, 1533, (2004)

9) K. Fujiwara, H.Monjushiro, H. Watarai, *Chem. Phys. Lett.*, **394**, 349 (2004).

10) Y. Matsumoto, H. Watarai, *Solv. Extr. Res. Dev. Jpn.*, **13**, 207 (2006).

11) H. Watarai, K. Sasaki, K.Takahashi, and J. Murakami, *Talanta*, **42**, 1961 (1995).

12) H. Watarai, K. Takahashi, and J. Murakami, *Sov. Extr. Res. Dev. Jpn.*, **3**, 109 (1996).

13) H. Nagatani, and H. Watarai, *Chem. Lett.*, **1997**, 167.

14) Y. Yulizar, A. Ohashi, and H. Watarai, *Anal. Chim. Acta.*, **447**, 247 (2001).

15) H. Watarai, K. Satoh, *Langmuir*, **10**, 3913 (1994).

16) H. Watarai, M. Gotoh, N. Gotoh, *Bull. Chem. Soc. Jpn.*, **70**, 957 (1997).

17) H.Nagatani, H. Watarai, *Anal. Chem.*, **70**, 2860 (1998).

18) A. Ohashi, H. Watarai, *Anal. Sci.*, **17**, 1313 (2001).

19) Y. Yulizar, A. Ohashi, H. Nagatani, H.Watarai, *Anal.Chim. Acta.*, **419**, 107 (2000).

20) N. C. Maiti, S. Mazumdar, N. Periasamy, *J. Phys. Chem. B*, **102**, 1528 (1998).

21) S. Okada, H. Segawa, *J. Am. Chem. Soc*. **125**, 2792 (2003).

22) S. Jeorge, I. Goldberg, *Acta Cryst.*, **61**, 1441 (2005).

23) J. S. Hu, Y. G. Guo, H. P. Liang, L. J. Wan, L. Jiang, *J. Am. Chem. Soc.*, **127**, 17090 (2005).